Article

Advances in Structural Engineering

Advances in Structural Engineering
2017, Vol. 20(10) 1523–1539

DOI: 10.1177/1369433216683197
journals.sagepub.com/home/ase
SAGE

Optimal distribution of friction dampers for seismic retrofit of a reinforced concrete moment frame

Jinkoo Kim and Seeun An

Abstract

This study investigated the story-wise optimal distribution of friction dampers to effectively reduce the seismic response of a reinforced concrete structure designed without considering seismic load. To this end, a genetic algorithm process was applied and the results were compared with those obtained by simple intuitive method based on story drift. The seismic performance of the model structure with optimally positioned friction dampers was evaluated by nonlinear static and dynamic analyses. The analysis results showed that compared with the system without friction dampers, the maximum roof displacement and the inter-story drift ratio were reduced by about 30% and 40%, respectively, after installation of the dampers. In comparison with the intuitive method of installation, the genetic algorithm provided an efficient solution for optimum damper distribution with less amount of friction damper.

Keywords

friction dampers, genetic algorithm, moment frames, optimum design, seismic retrofit

Introduction

In recent years, various passive energy dissipation devices have been applied for seismic retrofit of structures throughout the world. Among the passive dampers, friction dampers are one of the most frequently applied devices due to their effectiveness of energy dissipation and relative easiness of manufacturing. Mualla and Belev (2002) developed a rotational friction damper and showed that the hysteretic behavior of the friction damper was frequency-independent. Kim et al. (2011) investigated the effect of rotational friction dampers on enhancing seismic and progressive collapse resisting capacity of structures. Patel and Jangid (2011) investigated the dynamic response of adjacent structures connected by friction dampers. Kaur et al. (2012) compared the seismic performance of a steel moment-resisting frame with friction dampers with those of a moment frame and a braced frame. Beheshti-Aval et al. (2013) developed a hybrid friction-yielding damper for concentrically braced steel frames. Choi and Kim (2014) investigated the energy dissipation effect of friction dampers in coupling beams of reinforced concrete (RC) shear walls.

For application of passive dampers in multi-story structures, it is essential to determine the appropriate location and damping force in the structure. Many research works have been conducted to find out efficient damper distribution techniques throughout the stories. Zhang and Soong (1992) developed a sequential procedure for optimal placement of viscoelastic dampers by locating them in a story with maximum inter-story displacement. Gluck et al. (1996) developed an optimal damper allocation procedure based on active control theories. Takewaki (1997) developed an efficient method for application of energy dissipation devices based on minimizing the sum of amplitudes of the transfer functions of inter-story drifts evaluated at the undamped fundamental natural frequency of a structural system. Takewaki (2009) introduced an optimal performance–based design procedure of structures for earthquakes using passive dampers. Fujita et al. (2010) proposed a gradient-based optimization methodology for optimal design of viscous dampers to minimize an objective function defined for a linear structure. Martínez et al. (2013) used the sequential quadratic programming method and proposed a new objective function to find

Department of Civil and Architectural Engineering, Sungkyunkwan University, Suwon, Korea

Corresponding author:
Jinkoo Kim, Department of Civil and Architectural Engineering, Sungkyunkwan University, Suwon 440-746, Korea.
Email: jkim12@skku.edu

the optimal damper design based on the base moment in planar steel frames. Adachi et al. (2013) proposed an optimum design procedure for framed structures based on sensitivity analysis using nonlinear time history response analyses. Murakami et al. (2013) proposed a practical method for simultaneous optimal use of oil and dampers by formulating an optimum design problem to minimize the maximum inter-story drift under design earthquakes. Uz and Hadi (2014) carried out an optimal design of semi-active control system for adjacent buildings connected by magnetorheological (MR) damper based on integrated fuzzy logic and multi-objective genetic algorithm (GA).

For low-rise structures dominated primarily by the fundamental mode of vibration, simple intuitive methods for story-wise distribution of dampers may be applicable. However, for medium to high-rise structures with strong participation of higher vibration modes, more sophisticated optimization algorithm for damper distribution is required. One of the efficient methods used for optimum design of structures is the GA, which is a robust optimization technique based on the principles of natural biological evolution. GA has been applied for optimum design of structures (Hultman, 2010; Rajeev and Krishnamoorthy, 1997). Moreschi and Singh (2003) applied the GA to calculate the optimum design parameters of metallic and friction dampers to satisfy a pre-selected design objective. Movaffaghi and Friberg (2006) applied the GA-based method for the optimal damper placement of a given number of passive viscoelastic dampers in a nuclear power plant in order to reduce the acceleration responses at a nuclear reactor. Arfiadi and Hadi (2011) applied the hybrid-coded GA to optimize placement and properties of tuned mass dampers. All of the previous studies confirm that GA is a robust and reliable method for optimum damper distribution in building structures.

In this study, GA method was applied for optimum friction damper distribution in a 15-story RC structure with relatively long fundamental natural period in its longitudinal direction to minimize seismic responses. To estimate the range of friction damping effective in reducing earthquake response of the model structure as a preliminary study for optimal damper distribution, parametric study was carried out using an equivalent single-degree-of-freedom (ESDOF) system derived from the original structure. As huge amount of nonlinear time history analysis of the structure was involved in the GA procedure, the model structure was transformed into a simplified 15-degrees-of-freedom (DOF) system with similar dynamic characteristics. The results of optimum damper distribution obtained from GA were compared with those obtained by simple intuitive method based on story drift distribution. Finally, the limitations of this study were stated and recommendations were made for practical application of the optimization process in the conclusion.

Structural design of the case study structure

The analysis model structure to be retrofitted with friction dampers is a 15-story RC apartment building built in early 1970s. The structure is composed of moment-resisting frames in both directions and has uniform story height of 2.65 m. The structure has a rectangular plan shape with 5 m span length along the transverse direction and 3.35 and 3.55 m span length along the longitudinal direction as shown in Figure 1. As no structural information is available except the geometry and member sizes, the structure was re-designed to resist wind load as well as gravity load. The exterior corridor and the balcony, which were cantilevered from the slab along the longitudinal direction, were not considered in the structural modeling, but were included as line load along the exterior beams. The slabs were assumed to be rigid diaphragms and the strengths of RC and re-bars were assumed to be 21 and 400 MPa, respectively. The columns and beams in three consecutive stories were designed using the same elements. Considering the low story height, the depth of floor beams was limited to 35 cm. The size and re-bar placement in the structural elements in the first story are shown in Table 1. The fundamental natural period of the model structure turned out to be 2.7 s along the longitudinal direction and 2.3 s along the transverse direction.

Seismic performance of model structure

The seismic performance of the model structure designed only for wind and gravity loads was evaluated using the seismic performance criteria of ASCE/SEI 41 (2006). Nonlinear static analysis was carried out using the program code PERFORM-3D (2006). The nonlinear bending moment versus rotation relationships of beams and columns were represented by tri-linear lines as shown in Figure 2. The post-yield stiffness varies depending on the axial force as specified in the ASCE/SEI 41-06. Following the recommendation of ASCE/SEI 41-06, the over-strength factors of 1.5 and 1.25 were applied for the strength of RC and re-bars, respectively. The effective stiffness of beams and columns in elastic range was reduced to $0.5E_cI_g$ and $0.7E_cI_g$, respectively, considering cracked section. The shear strength of the elements was reduced to $0.4E_cA_w$.

Pushover analyses were carried out along the longitudinal and the transverse directions using lateral load

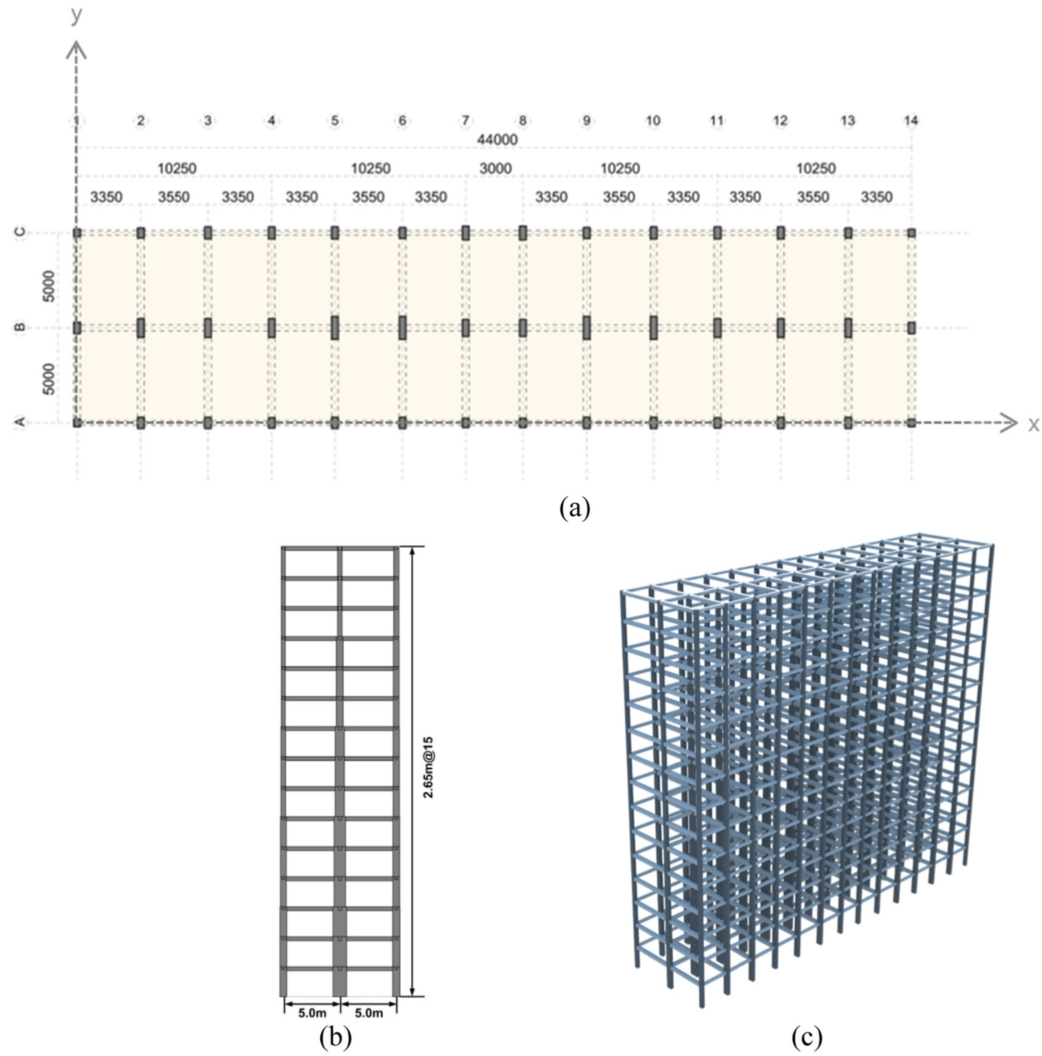

Figure 1. Configuration of the model structure: (a) structural plan, (b) elevation view, and (c) 3D view.

proportional to the fundamental mode shape of the structure in each direction. The lateral loads were applied until the roof displacements reached 4% of the building height, and the base shear versus roof displacement curves were plotted in Figure 3. The points corresponding to the design base shear, yield point, and the maximum inter-story drift of 2% are indicated on the pushover curves. The design base shears were obtained from ASCE 7-10 using the design spectral acceleration coefficients $S_{DS} = 0.49$ and $S_{D1} = 0.28$. These seismic coefficients were obtained based on the maximum considered earthquake (MCE) level ground acceleration of 0.22 g on class D site in Seoul area. It can be observed that the strength along the longitudinal direction is significantly smaller than the strength along the transverse direction, even smaller than the design base shear. This is due to the fact that the design wind load along the transverse direction is much higher than that along the longitudinal direction, and the seismic load was not considered in the design. It was observed that when loaded along the longitudinal direction, plastic hinges first formed at the beams in the mid-height and subsequently spread throughout the stories. The strength rapidly decreased when plastic hinges formed at the columns in the 10th and 11th stories. Based on the pushover analysis results, it was concluded that the model structure, which was designed without consideration of seismic load, needed seismic retrofit along the longitudinal direction.

Determination of effective friction damping

In this section, the range of friction damping effective in reducing earthquake response of the model structure was determined as a preliminary study for optimal damper distribution. To reduce the computation time

Table 1. Size of the first story beams and columns (mm).

Beams			
Name	Beam size (width × depth)	Re-bar	
		Ends	Middle
GA	250 × 250	2-D16	2-D16
GB	330 × 300	2-D19	2-D19
GC	250 × 250	2-D16	2-D16
G1	330 × 350	4-D22	2-D22
G2–6	350 × 350	6-D22	4-D22
G7	330 × 350	6-D22	2-D22
Columns			
Name	Size (width × depth)	Re-bar	
		Main	Tie
CA1	350 × 400	8-3 D19	D10@250
CA2–3	350 × 600	8-3 D29	D10@400
CA4	350 × 550	8-3 D25	D10@400
CA5–6	350 × 600	8-3 D29	D10@230
CA7	350 × 500	8-3 D25	D10@400
CB1	350 × 600	8-3 D25	D10@370
CB2–3	350 × 1000	12-3 D29	D10@210
CB4	350 × 1000	12-3 D29	D10@210
CB5–6	350 × 1200	12-3 D32	D10@400
CB7	350 × 900	12-3 D29	D10@400

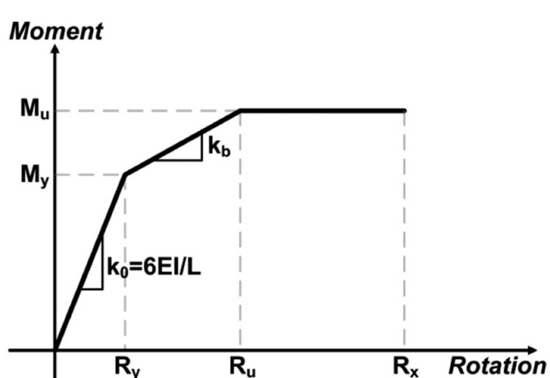

Figure 2. Nonlinear bending moment—chord rotation model of beams and columns.

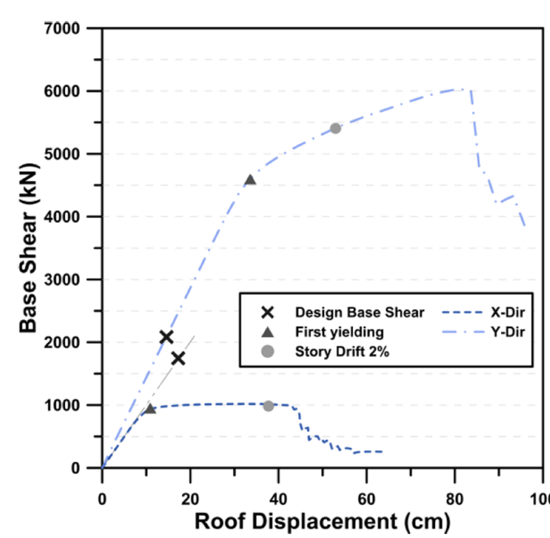

Figure 3. Nonlinear static pushover analysis result of the model structure.

required for nonlinear dynamic analysis, parametric study was carried out using an ESDOF system derived from the original structure using the following formulation

$$M_1^* = \frac{\left(\sum_{j=1}^{n} m_j \varphi_{j1}\right)^2}{\sum_{j=1}^{n} m_j \varphi_{j1}^2} \quad T_{eff} = 2\pi\sqrt{\frac{S_d}{S_a g}} \tag{1}$$

where M_1^* is the effective modal pass; m_j and φ_{j1} are the mass and the mode shape coefficient of the jth story, respectively; S_d and S_a are the spectral displacement and acceleration corresponding to the fundamental mode of vibration, respectively; and T_{eff} is the effective natural period of the first mode of vibration.

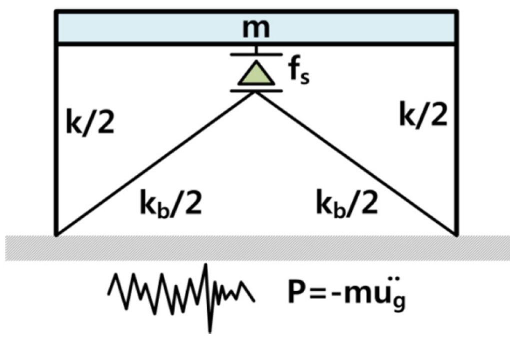

Figure 4. ESDOF with a friction damper and connecting braces.

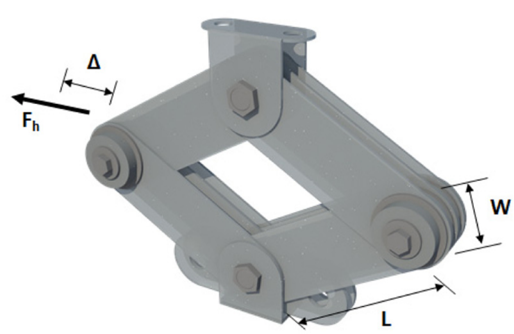

Figure 5. Typical configuration of a friction damper (Damptech, 2014).

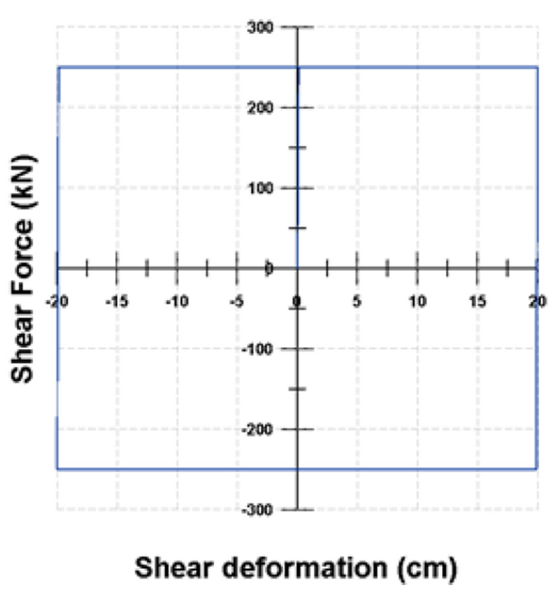

Figure 6. Hysteresis curve of a friction damper (F_h = 250).

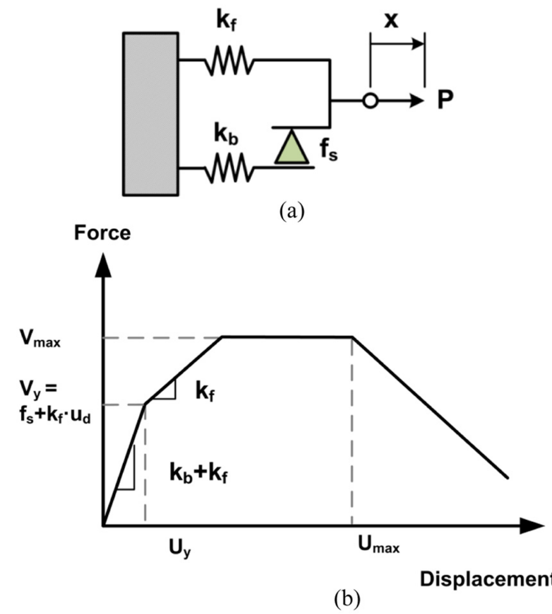

Figure 7. Modeling of the ESDOF structure with friction damper: (a) mathematical modeling and (b) force–displacement relationship.

The effective stiffness can be obtained from the above equation. The configuration of the ESDOF system with a friction damper is depicted in Figure 4, which is composed of the structure with stiffness k_f and the damper unit of a friction damper and connecting braces. Figures 5 and 6 show the typical configuration and hysteresis curve of a friction damper used in the seismic retrofit of building structures, respectively. Figure 7 depicts the idealized modeling and the force–displacement relationship of the equivalent system with a damper used in the analysis. In the modeling of the damper, f_s is the slip force of the friction damper and k_b is the stiffness of the connecting brace. The initial stiffness is contributed from the combined action of the structure and the damper, while only the structure resists the additional load after yielding of the friction damper. The pushover curve of the ESDOF system is compared with that of the original model structure in Figure 8, where it can be found that the two curves match reasonably well considering the simplicity of the ESDOF model. To confirm the validity of the ESDOF system, nonlinear dynamic analyses of the original and the ESDOF system were carried out using the three earthquake records selected from the database provided in the Pacific Earthquake Engineering Research (PEER) Center. The peak ground acceleration (PGA) and peak ground velocity (PGV) of the earthquake records used in the analysis can be found in Table 2. Figure 9 compares the top-story displacement time histories of the original and the ESDOF system obtained from the analysis. Even though the two responses generally coincide well with each other in terms of the maximum values, some discrepancy can be observed

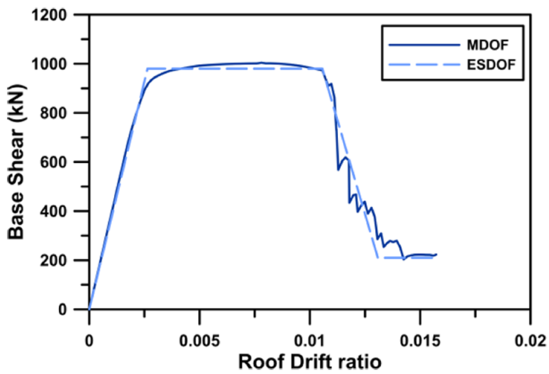

Figure 8. Nonlinear force–displacement curves of the original and the ESDOF system.

especially in the residual displacements. However, considering the simplicity of the ESDOF system and the fact that the seismic performance limit state is generally defined as the maximum inter-story drift, the use of the simplified system seems to be valid.

To find out the trend between added damping and structural responses and to determine the effective range of added friction damping to be used in the optimization process using GA, parametric study was conducted with the ESDOF system. The purpose of this stage was to determine the practical range of friction force to minimize the computation time required for the GA. The maximum displacements and the dissipated energy of the ESDOF system averaged over the three time history analysis results are plotted in Figure 10 for various slip force of the friction damper. The horizontal axis represents the ratio of the slip force of the friction damper and the design base shear. Two types of connecting brace stiffness were applied: brace stiffness equal to and twice the stiffness of the structure. The parametric study showed that the maximum displacement decreased significantly as the slip force exceeded 10% of the design base shear. When the stiffness of the connecting braces increased, the mean maximum displacement of the system decreased and the dissipated energy increased. The figure shows that when the stiffness of the connecting braces is twice the system stiffness, the displacement response is the minimum in case the slip force is about 25% of the design base shear. Also, the total dissipated energy is highest when the slip force is between 10% and 25% of the base shear. It can also be noted that when the stiffness of the connecting brace is twice the stiffness of the single-degree-of-freedom (SDOF) structure, the dissipated energy increased slightly. It was observed that as the stiffness of the connecting braces further increased more than twice the stiffness of the structure, the decrease in the maximum displacement and the increase in the dissipated energy were only marginal. Based on the parametric study presented in this section, the total damping force was restricted within $0.1 \leqslant \rho \leqslant 0.4$ and the stiffness of the connecting braces was kept twice of the story stiffness in the following optimization process for dampers.

Story-wise distribution of friction dampers

Distribution of dampers using GA

GA is an effective search technique based on natural selection having advantage in that it is simple to apply and can easily be modified for a broad field of problems. Theories on GA are well documented in many references (e.g. Rothlauf, 2006; Sivanandam and Deepa, 2008). The basic idea is to combine good solutions to a certain problem over many generations to

Table 2. Characteristics of the earthquake records used in the dynamic analysis.

Ground motion record	PGA (g)	PGV (cm/s)
Northridge NORTHR/LOS270	0.48	45
Hector Mine HECTOR/HEC000	0.34	42
Imperial Valley IMPVALL/H-E11140	0.38	42
Kobe, Japan KOBE/MIS090	0.51	37
Kobe, Japan KOBE/SHI000	0.24	38
Kobe, Japan KOBE/SHI090	0.24	38
Landers LANDERS/YER360	0.24	52
Superstition Hills SUPERST/B-ICC000	0.36	46
Superstition Hills SUPERST/B-POE270	0.45	36
Superstition Hills SUPERST/B-POE360	0.45	36
Cape Mendocino CAPEMEND/RIO270	0.55	44
Chi-Chi, Taiwan CHICHI/TCU045-N	0.51	39
San Fernando SFERN/PEL090	0.21	19

PGA: peak ground acceleration; PGV: peak ground velocity.

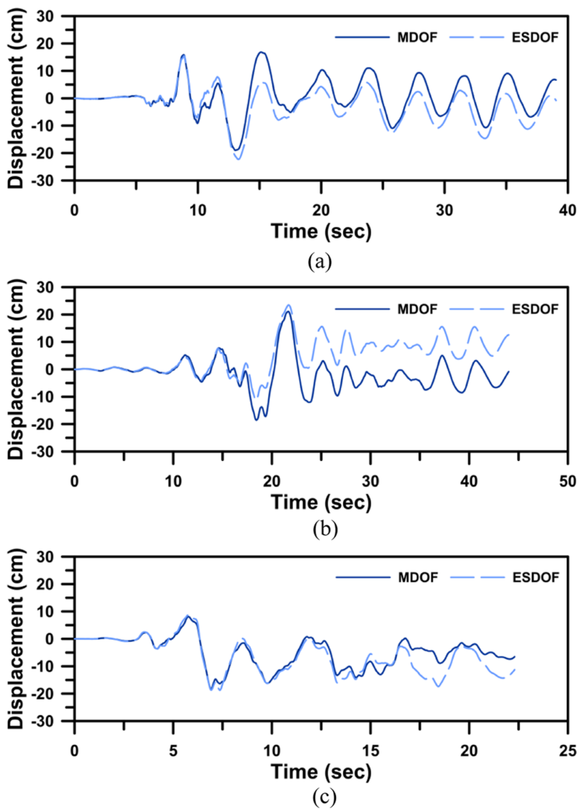

Figure 9. Comparison of time history curves of ESDOF model and MDOF model: (a) Imperial Valley, (b) Landers, and (c) Superstition Hills.

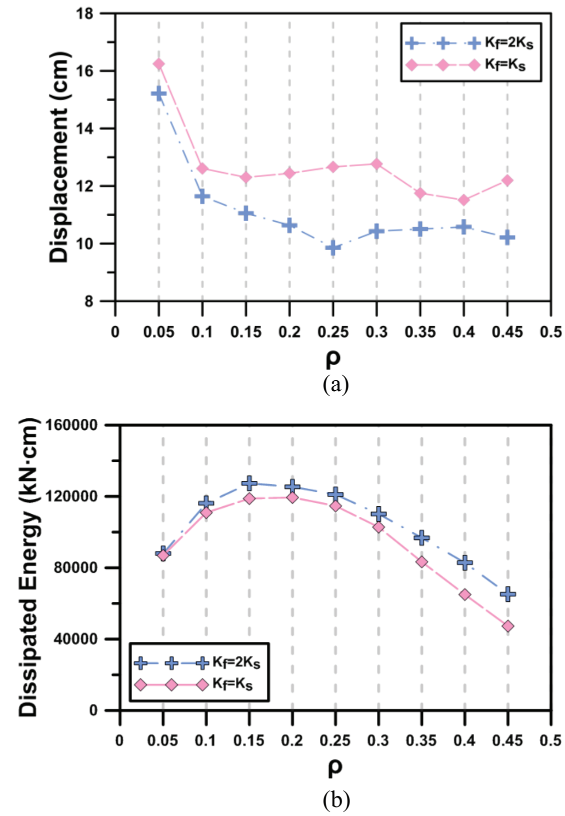

Figure 10. Response of the structure with friction dampers for various slip force ratios: (a) maximum displacement and (b) dissipated energy.

gradually improve the result. All solutions are initially created randomly, and they are individually represented by a binary string. The breeding operation continues until a certain number of generations are exceeded or no further improvement is achieved. GA has basic operators such as selection, crossover, and mutation, which are applied on a population in each generation to improve their fitness. Generations are reproduced by selecting individuals with good fitness which is determined by an objective function. In this article, the roulette wheel selection was used to create next generation (Rothlauf, 2006), in which a proportion of the wheel is assigned to each of the possible selections based on their fitness value. This could be achieved by dividing the fitness of a selection by the total fitness of all the selections, thereby normalizing them to 1. Then, a random selection is made similar to how the roulette wheel is rotated. To create a better population, two random individuals from the mating pool are chosen as parents, and some portion of their strings are cut and switched to create two children. To prevent the algorithm from getting stuck in a local minimum, a mutation process is applied to an individual by changing a bit in the string from 0 to 1 or vice versa (Sivanandam and Deepa, 2008).

In this study, the optimum story-wise distribution of damper slip force to minimize structural responses was considered as the main design variable to be optimized using GA. It was assumed that the dampers were installed along the longitudinal direction at locations where they did not affect the symmetry of the structure. Since huge number of nonlinear time history analyses were involved in the optimization process using GA, the use of the 15-story full-scale model structure was almost impossible. To reduce the computation time significantly, the model structure was transformed into an equivalent 15-DOF system as shown in Figure 11. The stiffness of each story of the equivalent structure, shown in Figure 12, was obtained from the story shear versus inter-story drift relationships of the original structure. Figure 13 shows the roof displacement time histories of the original and the simplified models obtained from the nonlinear time history analysis using the Northridge earthquake (PGA = 0.52 g). Even though the two results are not identical, the simplified model represents the maximum value reasonably well.

Figure 14 depicts the flow chart of the optimizing story-wise damper distribution in the 15-DOF system

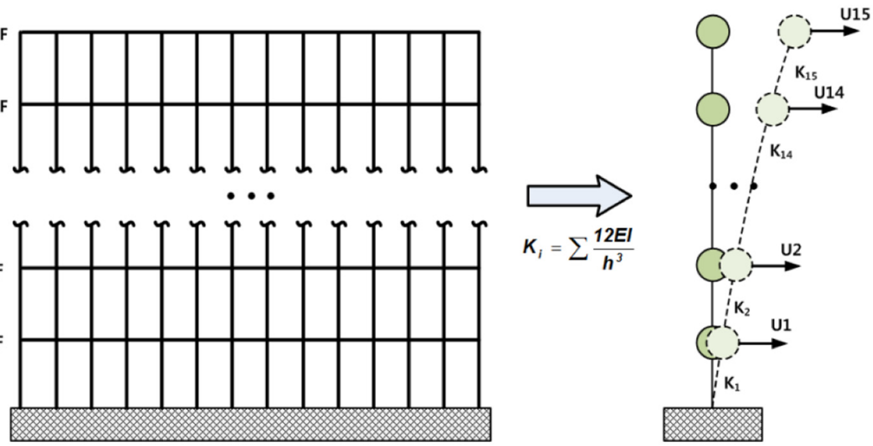

Figure 11. 15-degrees-of-freedom system idealization of the model structure.

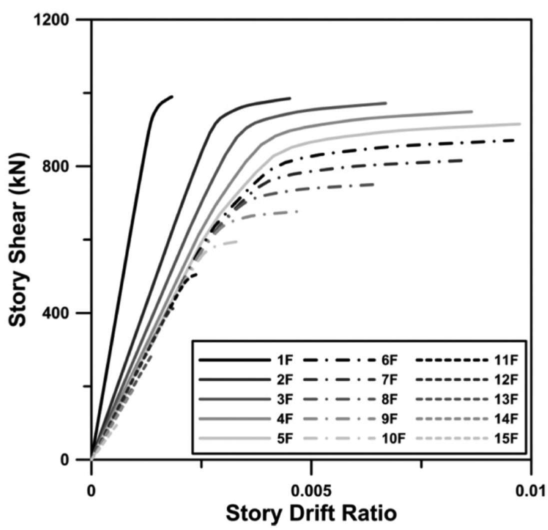

Figure 12. Story stiffness of the model structure obtained from pushover analysis.

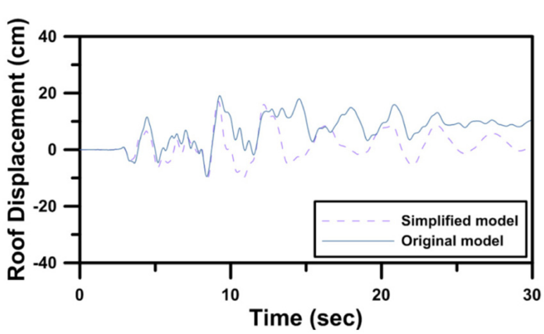

Figure 13. Comparison of roof displacement time histories of original and simplified models (Northridge earthquake, PGA = 0.52 g).

using GA. In the first step of the optimization process, a number between 1 and $(2^{15}-1)$ was randomly selected and was changed to binary number. The binary number was allocated to a string or a gene composed of 15 bits which represent the DOFs (or each story) of the structure. The bits allocated with the number "1" represent the stories with dampers and those with "0" represent the stories without dampers. Therefore, each string allocated with distinct binary number represents different damper distribution patterns. In the second step, a random number between 100 and 800, which implies the slip force of the friction damper in kilonewton, was put to each story allocated with the number "1." In this study, a total of 1000 strings containing different information about story-wise distribution of damper slip force were randomly generated and were put into breeding process over 100 generations until optimum solution was derived. In the third step, the fitness value of each string of damper distribution was evaluated by nonlinear time history analysis of the 15-DOF system using Northridge earthquake record. To this end, the structural responses such as the maximum inter-story drift, the summation of all inter-story drifts, and the maximum top-story displacement were considered as performance indices to be minimized. The fitness value $F_{fitness}$ was computed for the two performance indices, GA1 and GA2, as follows

$$F_{fitness} = \frac{\sum_i^n D_{O,i}}{\sum_i^n D_{D,i}} + \frac{D_{O,\max}}{D_{D,\max}} + \frac{D_{RO,\max}}{D_{RD,\max}} \quad \text{(GA1)} \quad (2)$$

$$F_{fitness} = \frac{\sum_i^n D_{O,i}}{\sum_i^n D_{D,i}} + \frac{D_{O,\max}}{D_{D,\max}} + \frac{D_{RO,\max}}{D_{RD,\max}} + \left(1 - \frac{n_f}{n}\right) \quad \text{(GA2)} \quad (3)$$

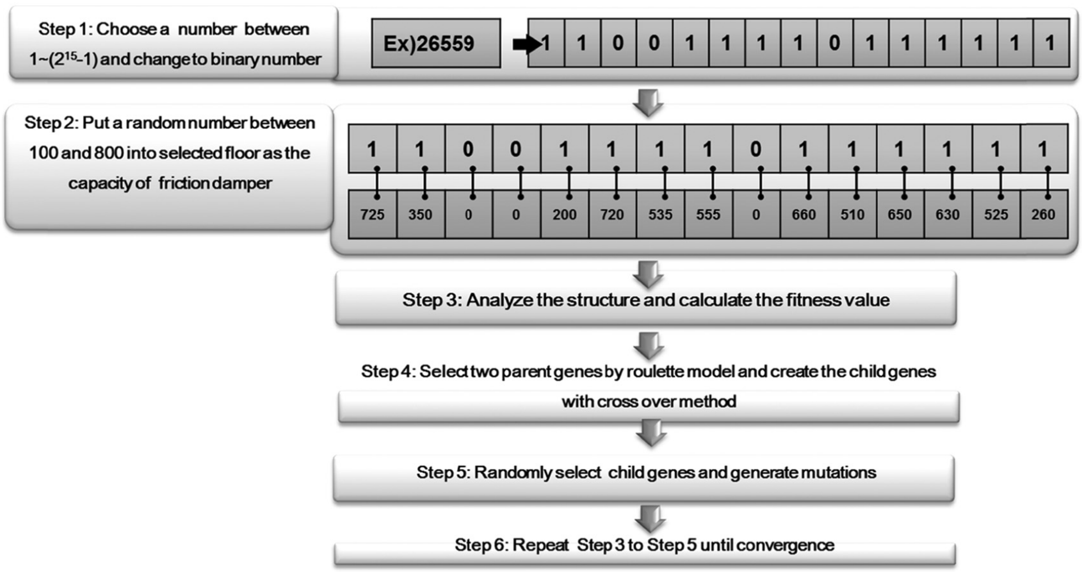

Figure 14. Flow chart of genetic algorithm applied in this study.

where $D_{O,i}$ and $D_{D,i}$ are the inter-story drifts of the ith story without and with dampers, respectively; $D_{O,\max}$ and $D_{D,\max}$ are the maximum inter-story drifts of the structure without and with dampers, respectively; $D_{RO,\max}$ and $D_{RD,\max}$ are the maximum roof story drifts of the structure without and with dampers, respectively; n_f and n are the number of stories with dampers and the total number of stories, respectively. It can be observed that the performance indices are similar to each other except that the number of stories with dampers is included in the index GA2. In the fourth step, the second-generation genes were reproduced from the parent genes using the fitness-proportionate selection method known as the roulette wheel selection method, which is a genetic operator for selecting potentially useful solutions for recombination. In this method, a circle was divided into 1000 sectors, which is the number of individual damper distribution schemes. The arc of each sector was kept proportional to the selection probability P of the corresponding individual, which was calculated as the proportion of its fitness value to the sum of the fitness values of all individuals as follows

$$P(H_j) = \frac{f(H_j)}{\sum_{1}^{Ns} f(H_i)} \tag{4}$$

where $f(H_j)$ is the fitness value of the string H_j and N_s is the total number of strings which is 1000 in this study. This means that strings with greater fitness are more likely to be selected than strings with lesser fitness. In this way, the optimum damper distribution pattern is gradually selected which minimizes the given performance objectives GA1 and GA2.

Once two parent genes were selected by the roulette wheel selection method, some portion of their strings were switched to create two children genes. This process is called crossover, which is a convergence operation intended to pull the population toward a local minimum/maximum. In this study, the single-point crossover operation was conducted 1000 times to generate a total of 1000 second-generation genes. In the fifth step, a string was randomly selected from the second-generation genes and was mutated in such a way that each bit in the string was changed from 0 to 1 or vice versa. This process is called mutation which is a divergence operation intended to occasionally break one or more members of a population out of a local minimum/maximum space so that the algorithm was not trapped in a suboptimal local value of the target performance objective. The process from step 3 to step 5 was repeated 100 times until the children genes (strings) in the 100th generation were reproduced through GA. Among the genes in the 100th generation, the one with the highest fitness value was chosen as the optimum solution for damper distribution.

Figure 15 shows the variation of the fitness values in the optimization process. It can be observed that for both the objective functions GA1 and GA2, the mean fitness value gradually converged to a certain value. It can also be noted that in the beginning of the optimization process, the fitness values are widely scattered; however, as the breeding operation continues, the scatter in the fitness value keeps decreasing. This implies that at the final stage of the GA, most of the genes

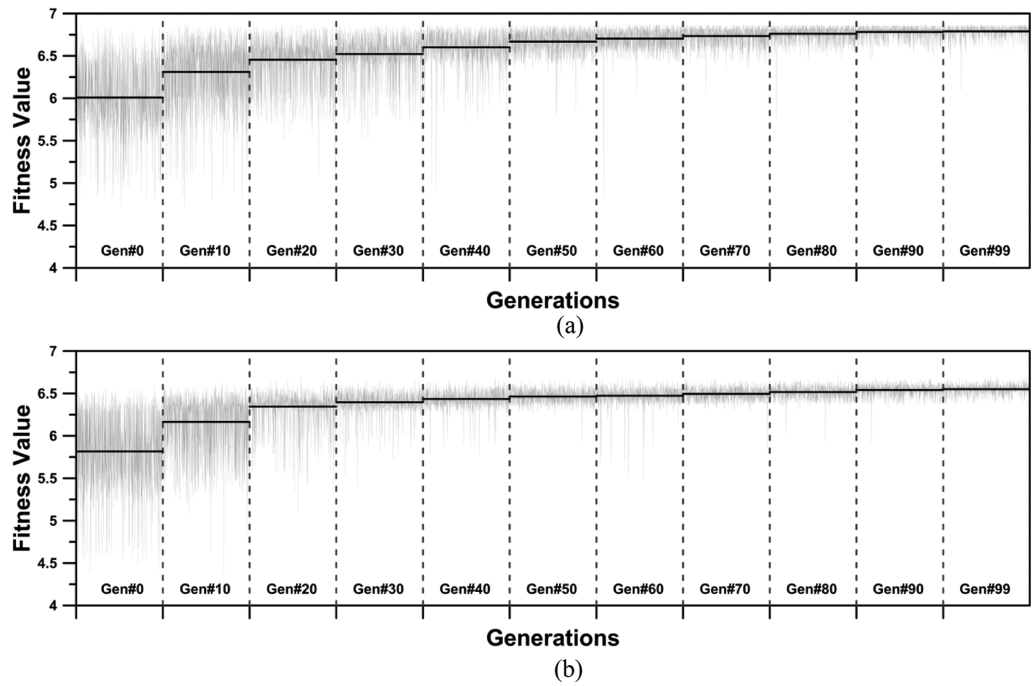

Figure 15. Variation of fitness values during the optimization process of genetic algorithm: (a) GA1 and (b) GA2.

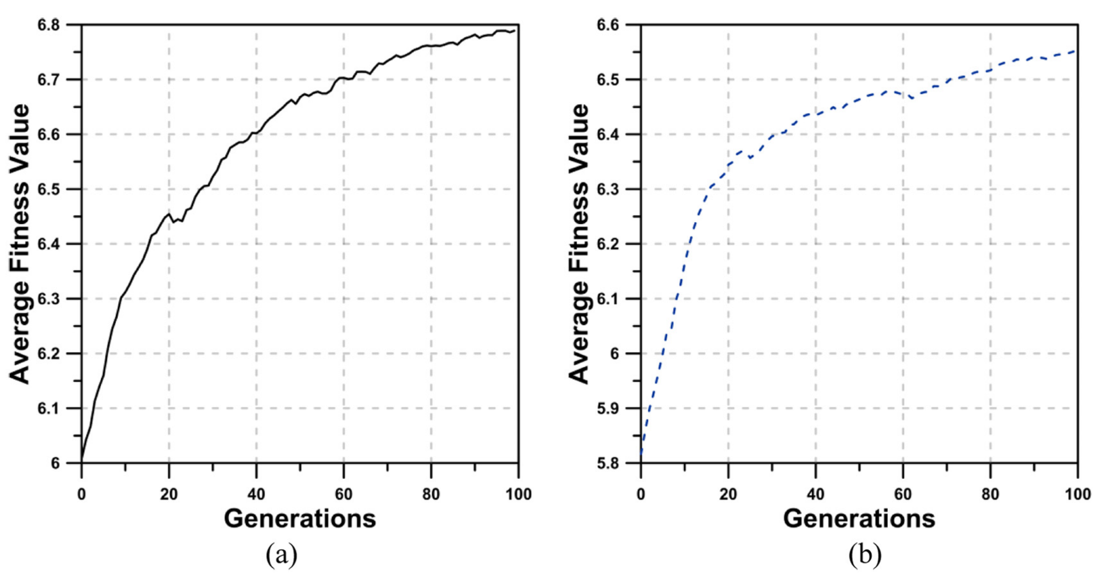

Figure 16. Variation of mean fitness value of two performance indices: (a) GA1 and (b) GA2.

reached near the optimum solution. Figure 16 depicts the mean fitness value of the two performance objectives as a function of the number of generations. The beginning and the final mean fitness values of the performance objective GA1 turned out to be slightly higher than those of the performance objective GA2. Figure 17 depicts the story-wise optimum distribution patterns of friction dampers obtained from the GA using the performance objectives GA1 and GA2. For GA1 performance objective, dampers were installed in every story, even though the number of story was not included specifically in the performance objective, whereas for GA2, which considers the number of stories with dampers as one of the performance objective, dampers were not installed in the upper two stories. The summation of slip force of all dampers of GA1

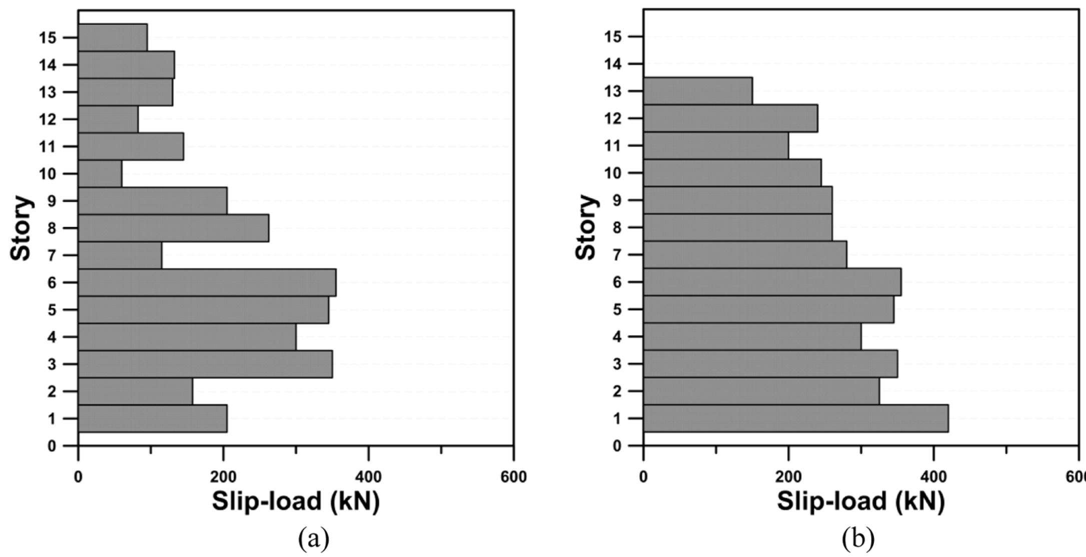

Figure 17. Distribution of friction dampers by genetic algorithm: (a) GA1 and (b) GA2.

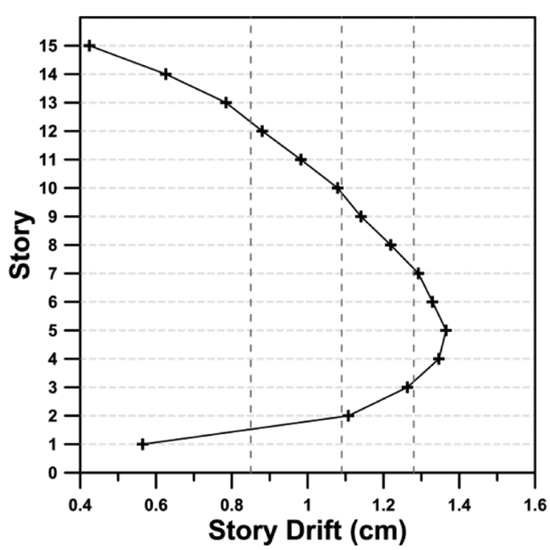

Figure 18. Story-wise distribution of inter-story drift of the model structure subjected to design seismic load.

and GA2 was 2940 and 7460 kN, respectively, which corresponded to $\rho = 0.12$ and 0.42, respectively.

Distribution of dampers using intuitive method

Marko et al. (2006) showed that friction dampers are most effective when placed close to regions of the maximum inter-story drift. Based on this finding, simple intuitive method for damper distribution based on inter-story drift was applied for comparison with the optimum damper distribution derived from GA. The slip force of the dampers installed in the ith story, $f_{s,i}$, was obtained as follows

$$f_{s,i} = F_{total} \frac{D_i}{\sum_{i=1}^{n} D_i} \tag{5}$$

where F_{total} is the total slip force of the dampers determined as a fraction of the design base shear and D_i is the inter-story displacement of the ith story. The inter-story drifts were obtained from the analysis of the original model structure subjected to the design seismic load and are presented in Figure 18. The dampers were installed at 4, 8, and 11 stories and the results were compared. Based on the parametric study shown in Figure 10, the total slip force varied from 10% to 30% of the design base shear. The resultant story-wise damper distributions at 8 and 11 stories are shown in Figures 19 and 20, respectively.

Response of the model structure with friction dampers

Pushover analysis results

To investigate the effect of added dampers on overall strength, nonlinear static pushover analyses of the model structure installed with friction dampers were carried out along the longitudinal direction using the nonlinear analysis program code PERFORM-3D. The maximum strength of the structure installed with friction dampers at 11 stories based on the inter-story drift turned out to be larger than the maximum strength of the structure with dampers installed at 4 and 8 stories.

It was observed that when the dampers were installed concentrated in four stories, they stopped yielding and the strength stopped increasing when ρ

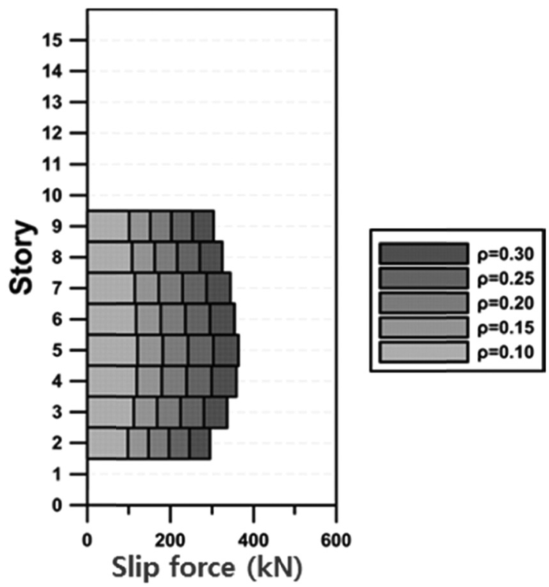

Figure 19. Distribution of friction dampers in eight stories based on story drift.

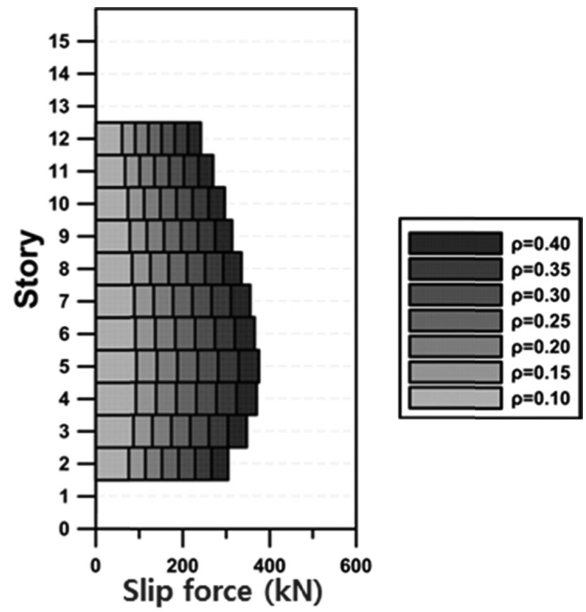

Figure 20. Distribution of friction dampers in 11 stories based on story drift.

was increased higher than 0.2. The strength increased to the highest level when the dampers were distributed to 11 stories. Figure 21 shows the pushover analysis results of the structure with dampers installed at 11 stories using the intuitive method, where it can be observed that as a result of installing dampers the strength of the model structure increased significantly. Even though the strength generally increased proportionally to the slip force ratio ρ, the strength started to decrease when ρ increased from 0.35 to 0.4. It was observed that when ρ exceeded 0.4, some dampers did not slip and inelastic deformation was concentrated in the beams, which leaded to sudden drop of strength.

Figure 22 compares the pushover curves of the model structure installed with friction dampers distributed by the GA1 (ρ = 0.12) and GA2 (ρ = 0.42) methods. In comparison with the results of the intuitive method presented in Figure 21, it can be observed that the damper distribution using the genetic algorithm GA1 resulted in 32% increase in the overall strength of the structure compared with the strength obtained from the simplified method with similar amount of damper slip force (ρ = 0.1). It can also be observed that GA2 produces similar result to the GA1, but with significantly larger damper slip force.

Time history analysis results

To investigate the seismic performance of the model structure with friction dampers installed by various methods, nonlinear dynamic analyses were carried out using the 13 earthquake records provided in the PEER. Among the database, the records with their spectral values at the natural period of the model structure within ±20% of the design-based earthquake (DBE) spectrum were selected. Table 2 shows the lists of the earthquake records used in the analysis, and Figure 23 depicts the response spectra of the 13 records and the design spectrum.

Figure 24 shows the maximum inter-story drift of each story of the model structure averaged over 13 nonlinear dynamic analysis results. The analysis results of the model structure installed with dampers distributed by the GA methods were compared with the story drifts of the original bare structure. It can be observed that the maximum average inter-story drift of 0.014 rad occurred at the sixth story of the bare frame. The inter-story drift at that story was minimized when the dampers were distributed by GA1 method. In the stories above the 13th floor, the inter-story drifts became minimized by the GA1 method.

Figure 25 shows the results of the parametric study for the maximum inter-story drift, sum of mean inter-story drift, and the maximum roof displacement of the model structure with dampers averaged over 13 nonlinear dynamic analysis results. The response quantities of the structure with dampers installed based on the inter-story drift at 4 (4F_D), 8 (8F_D), and 11 stories (11F_D) were plotted for various slip force ratios ρ. The results of the original structure without dampers are indicated as horizontal alternated long and short dash lines, and the results of genetic algorithms GA1 and GA2 are also shown in the figure. It

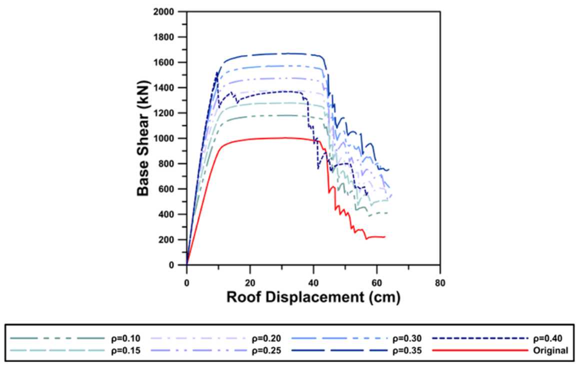

Figure 21. Pushover analysis results of the structure with dampers at 11 stories distributed based on story drift.

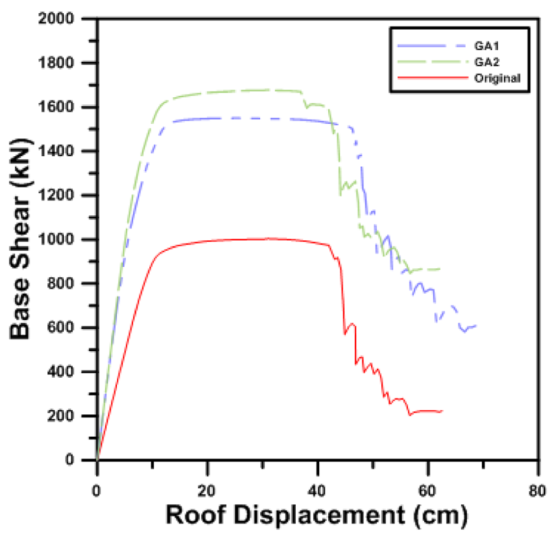

Figure 22. Pushover curves of the model structure with friction dampers distributed by genetic algorithm.

can be observed that the responses generally decreased as a result of the damper installation. However, in case the dampers were installed only at four stories, all responses increased even higher than those of the original structure when damper slip force ρ was 0.2. When dampers were installed in total of eight stories, the responses stopped decreasing or rather started to increase when ρ exceeded 0.25. Similar results were observed when ρ of dampers installed at a total of 11 stories exceeded 0.35. The distribution of dampers using the genetic algorithm GA1 and GA2 resulted in lower bounds of the response quantities. The results demonstrate the superiority of the GA method over the intuitive distribution procedure based on inter-story drift.

Figure 26 depicts the components of the dissipated energy in the model structure with dampers distributed

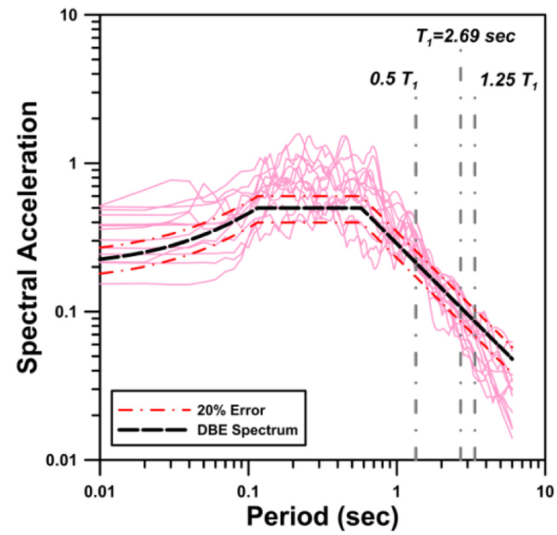

Figure 23. Response spectra of the earthquake records selected for time history analysis.

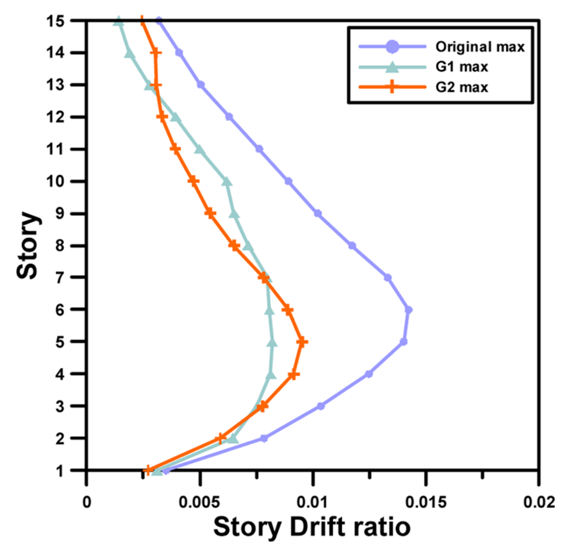

Figure 24. Mean inter-story drift ratio of the model structure without and with friction dampers obtained from nonlinear time history analyses using the 13 earthquake records.

by GA obtained from dynamic analysis using the 13 earthquake records. The average values of the dissipated energy in dampers are also plotted in the figure. It can be observed that seismic input energy was mostly dissipated by the dampers and the beams. The mean dissipated energy in the dampers contributed to 66% and 71% of the mean input energy in the structure with GA1 and GA2 damper distribution, respectively, and the dissipated energy in the structural elements is reduced to 51% and 60% of those in the original structure, respectively. The mean dissipated

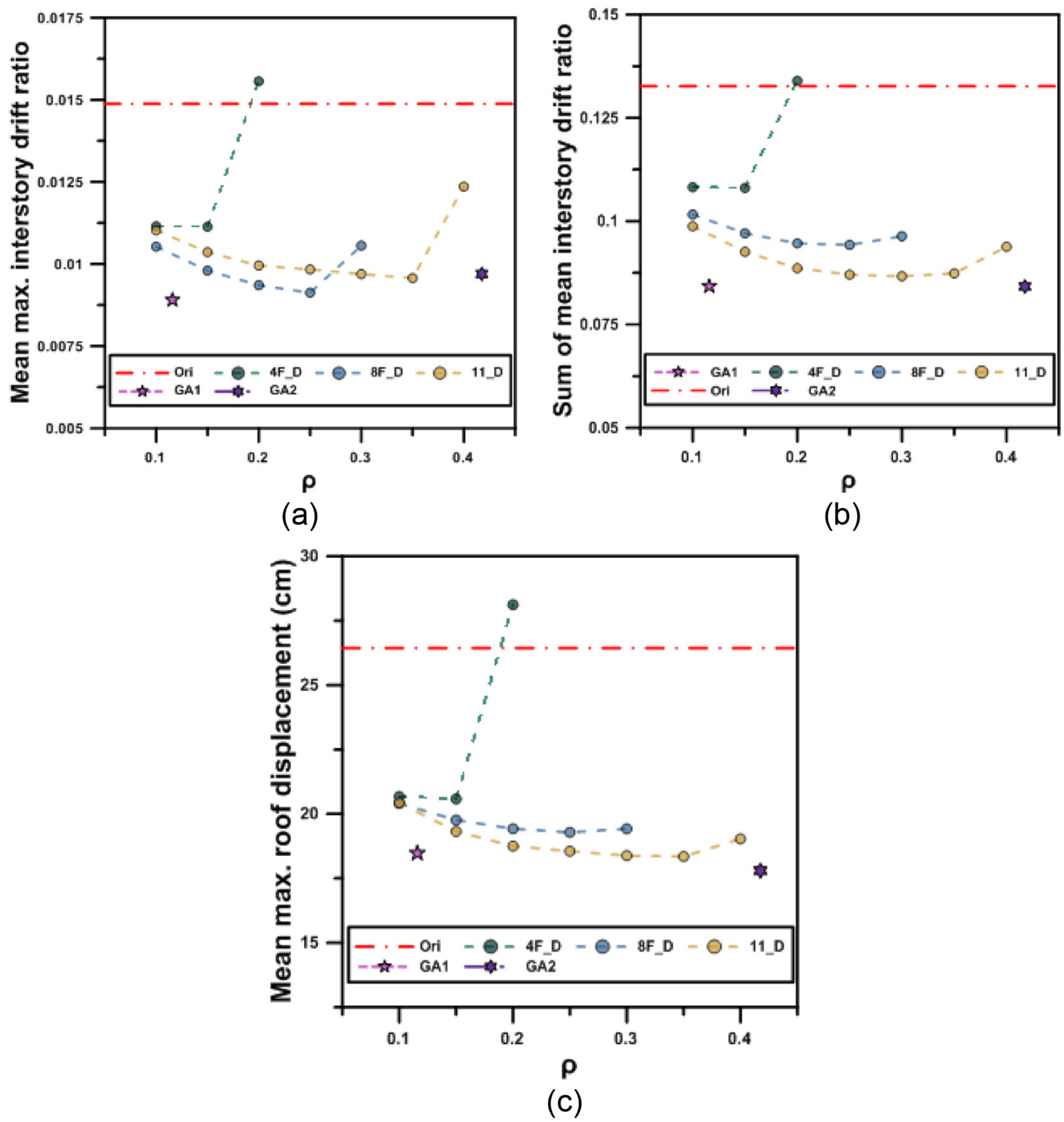

Figure 25. Nonlinear dynamic analysis results of the structure having friction dampers with various slip force ratios: (a) mean maximum inter-story drift ratio, (b) sum of mean inter-story drift ratio, and (c) mean maximum roof displacement.

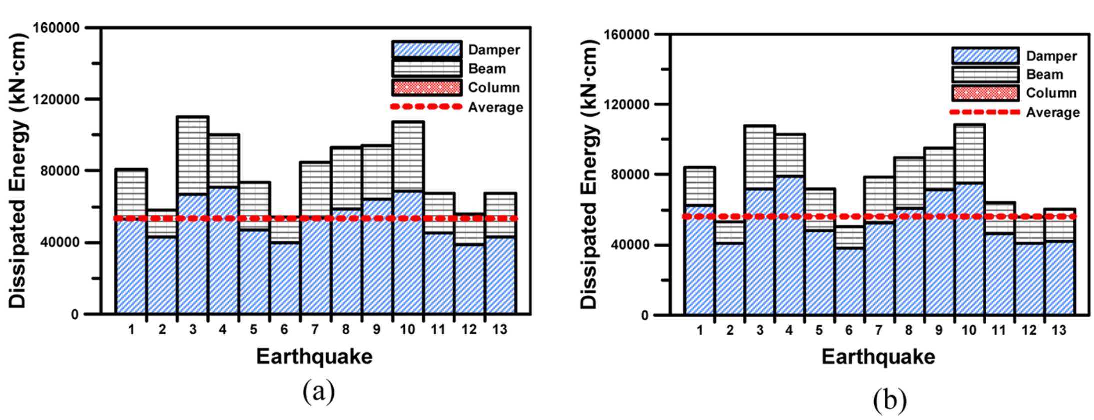

Figure 26. Energy dissipation in the structure with friction dampers distributed using genetic algorithm: (a) GA1 and (b) GA2.

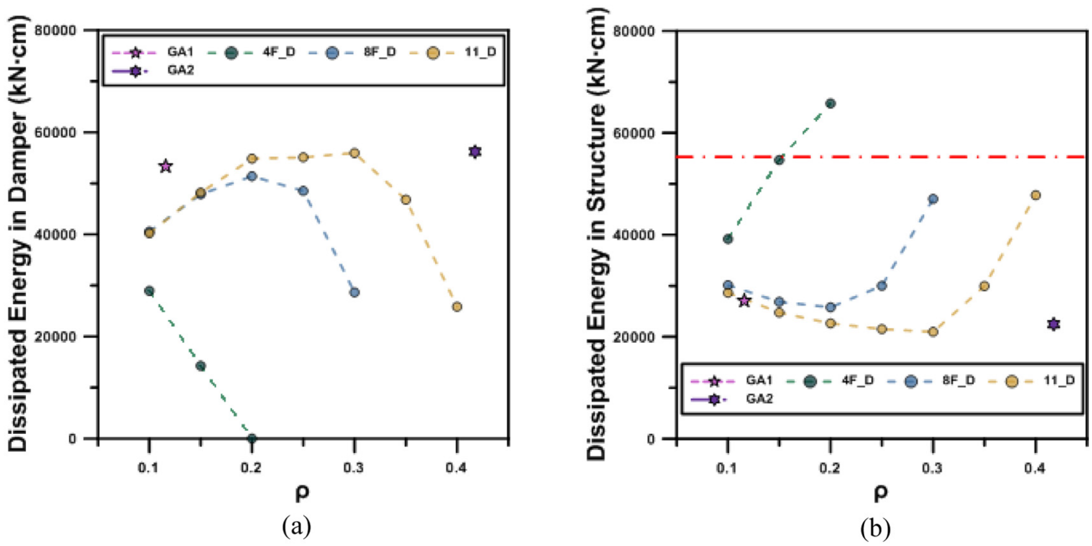

Figure 27. Energy dissipation in the structure having friction dampers with various slip force ratios: (a) energy dissipated by dampers and (b) energy dissipated by structure.

energy in the dampers was slightly higher in the structure with GA2 damper distribution. Figure 27 plots the mean dissipated energy in the dampers and the structure. When dampers were installed only in four stories based on the inter-story drift, the dissipated energy in the dampers decreased and the energy dissipated in the structure increased when ρ increased from 0.1 to 0.2. When dampers were distributed to 11 stories, the dissipated energy in the dampers increased until ρ reached 0.3, but then started to decrease as ρ further increased. The opposite was observed for the dissipated energy in the structure. The GA with GA1 performance index resulted in quite desirable seismic energy dissipation in the model structure with relatively small amount of damping force.

Figure 28 plots the variation of the performance index J determined by combining various response quantities as follows

$$J = \frac{E_{SD}}{E_{SO}} + \left(1 - \frac{E_F}{E_T}\right) + \frac{\sum_i^n D_{D,i}}{\sum_i^n D_{O,i}} + \frac{D_{D,\max}}{D_{O,\max}} + \frac{D_{RD,\max}}{D_{RO,\max}} \quad (6)$$

where n is the number of stories; E_{SD} and E_{SO} are the dissipated energy in the structural members in the structure with and without dampers, respectively; E_F and E_T are the dissipated energy in the friction dampers and the total dissipated energy, respectively; D_D and D_O are the inter-story drifts of the structure with and without dampers, respectively; D_{RD} and D_{RO} are the roof story drifts of the structure with and without dampers, respectively. It can be observed that the GA1 distribution of dampers provided smallest performance index with small slip force ratio of $\rho = 0.12$. However, the distribution of dampers using the genetic algorithm GA2 resulted in the smallest performance index at $\rho = 0.42$. Therefore, the inclusion of irrelevant constraints or performance objectives in the algorithm may lead to less economical solution. The distribution of dampers in 11 stories based on the inter-story drift produced slightly higher performance index at slip force ratio of $\rho = 0.25$–0.35. This implies that to achieve the same level of seismic performance, two to

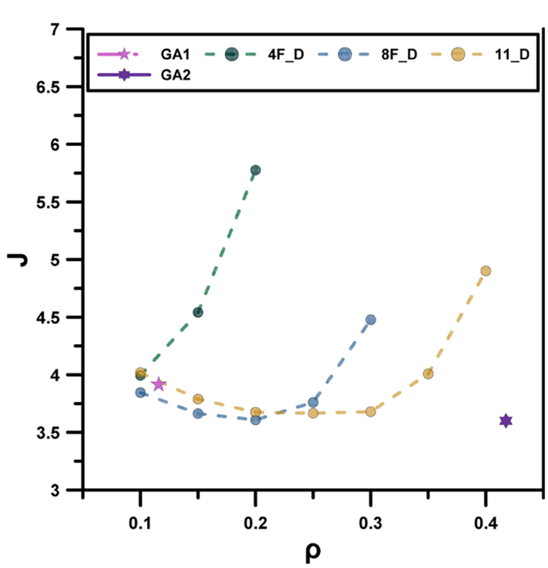

Figure 28. Performance index J for various slip force ratios.

three times larger slip force is required in the intuitive method. Even though the GA with proper constraints and/or performance objectives usually provides an optimum solution with maximum economy, huge computational demand associated with the algorithm often makes it impractical. Therefore, a series of parametric study based on proper understanding of seismic performance of structures may produce a near optimum solution for economic damper distribution throughout the stories.

Conclusion

This study investigated the optimal distribution of friction dampers using GA to effectively reduce the seismic response of a RC structure designed without considering seismic load. The range of friction damping effective in reducing earthquake response of the model structure was determined as a preliminary study for optimal damper distribution using an ESDOF system. Then, the original model structure was transformed into an equivalent multi-DOF system with one DOF in each story to reduce the computation time required for nonlinear dynamic time history analyses. The seismic performance of the model structure with optimally positioned friction dampers was evaluated by nonlinear static and dynamic analyses. The analysis results of the structure with friction dampers optimally distributed by GA were compared with those distributed by simple intuitive method based on story drift.

The analysis results showed that compared with the system without friction dampers, the maximum roof displacement and the inter-story drift ratio were reduced by about 30% and 40%, respectively, after installation of the dampers. Also, as high as about 70% of the earthquake input energy was dissipated by the dampers, and the energy dissipated in the structural elements was reduced by about 50%. The GA provided an efficient solution for optimum damper distribution with less amount of damper slip force in comparison with the intuitive method based on inter-story drifts. Therefore, it would be necessary to come up with a few alternatives for objective function and select the most reasonable solution. As huge amount of computation time is required for application of GA using nonlinear dynamic analysis, transformation of an original structure into an equivalent simplified structure with reduced DOFs is highly recommended in practice. Also, preliminary parametric study for estimating effective range of added damping using an equivalent SDOF system may further expedite the optimization process.

It should be pointed out that in this article, the optimum solution for story-wise damper distribution was obtained using single earthquake record, and more generalized solution can be achieved using more earthquake records in the optimization process. In addition, the validity of the optimization needs to be verified by proper test of a model structure installed with friction dampers distributed throughout the structure based on the procedure described in this study since the optimum solution may vary due to the discrepancy between the real structure and its analysis modeling.

Declaration of Conflicting Interests

The author(s) declared no potential conflicts of interest with respect to the research, authorship, and/or publication of this article.

Funding

The author(s) disclosed receipt of the following financial support for the research, authorship, and/or publication of this article: This research was supported by a grant (16AUDP-B066083-04) from Architecture & Urban Development Research Program funded by Ministry of Land, Infrastructure and Transport of Korean government.

References

Adachi F, Yoshitomi S, Tsuji M, et al. (2013) Nonlinear optimal oil damper design in seismically controlled multi-story building frame. *Soil Dynamics and Earthquake Engineering* 44(1): 1–13.

Arfiadi Y and Hadi MNS (2011) Optimum placement and properties of tuned mass dampers using hybrid genetic algorithms. *International Journal of Optimization in Civil Engineering* 1: 167–187.

ASCE/SEI 41 (2006) *Seismic Rehabilitation of Existing Buildings*. New York: American Society of Civil Engineers.

Beheshti-Aval SB, Mahbanouei H and Zareian F (2013) A hybrid friction-yielding damper to equip concentrically braced steel frames. *International Journal of Steel Structures* 13(4): 577–587.

Choi K and Kim HJ (2014) Strength demand of hysteretic energy dissipating devices alternative to coupling beams in high-rise buildings. *International Journal of High-Rise Buildings* 3(2): 107–120.

Damptech (2014) Available at: http://www.damptech.com/

Fujita K, Yamamoto K and Takewaki I (2010) An evolutionary algorithm for optimal damper placement to minimize interstorey-drift transfer function in shear building. *Earthquakes and Structures* 1(3): 289–306.

Gluck N, Reinhorn AM, Gluck J, et al. (1996) Design of supplemental dampers for control of structure. *Journal of Structural Engineering* 122(12): 1394–1399.

Hultman M (2010) *Weight optimization of steel trusses by a genetic algorithm—size, shape and topology optimization according to Eurocode*. Master's thesis, Department of Structural Engineering, Lund Institute of Technology, Lund.

Kaur N, Matsagar VA and Nagpa AK (2012) Earthquake response of mid-rise to high-rise buildings with friction dampers. *International Journal of High-Rise Buildings* 1(4): 311–332.

Kim J, Choi H and Min K (2011) Use of rotational friction dampers to enhance seismic and progressive collapse resisting capacity of structures. *Structural Design of Tall and Special Buildings* 20(4): 515–537.

Marko J, Thambiratnam D and Perera N (2006) Study of viscoelastic and friction damper configurations in the seismic mitigation of medium-rise structures. *Journal of Mechanics of Materials and Structures* 1(6): 1001–1039.

Martínez CA, Curadelli O and Compagnoni ME (2013) Optimal design of passive viscous damping systems for buildings under seismic excitation. *Journal of Constructional Steel Research* 90: 253–264.

Moreschi LM and Singh MP (2003) Design of yielding metallic and friction dampers for optimal seismic performance. *Earthquake Engineering & Structural Dynamics* 32: 1291–1311.

Movaffaghi H and Friberg O (2006) Optimal placement of dampers in structures using genetic algorithm. *Engineering Computations* 23(6): 597–606.

Mualla IH and Belev B (2002) Performance of steel frames with a new friction damper device under earthquake excitation. *Engineering Structures* 24(3): 365–371.

Murakami Y, Noshi K, Fujita K, et al. (2013) Simultaneous optimal damper placement using oil, hysteretic and inertial mass dampers. *Earthquakes and Structures* 5(3): 261–276.

Patel CC and Jangid RS (2011) Dynamic response of adjacent structures connected by friction dampers. *Earthquakes and Structures* 2(2): 149–169.

PERFORM-3D (2006). *Nonlinear Analysis and Performance Assessment for 3D Structures, User Guide*. Berkeley, CA: Computers and Structures.

Rajeev S and Krishnamoorthy CS (1997) Genetic algorithm based methodologies for design optimization of trusses. *Journal of Structural Engineering* 123: 350–358.

Rothlauf F (2006) *Representations for Genetic and Evolutionary Algorithms*. Berlin: Springer.

Sivanandam SN and Deepa SN (2008) *Introduction to Genetic Algorithms*. Berlin: Springer.

Takewaki I (1997) Optimal damper placement for minimum transfer functions. *Earthquake Engineering & Structural Dynamics* 26: 1113–1124.

Takewaki I (2009) *Building Control with Passive Dampers: Optimal Performance-based Design for Earthquakes*. Hoboken, New Jersey: John Wiley & Sons.

Uz ME and Hadi MNS (2014) Optimal design of semi active control for adjacent buildings connected by MR damper based on integrated fuzzy logic and multi-objective genetic algorithm. *Engineering Structures* 69: 135–148.

Zhang RH and Soong TT (1992) Seismic design of viscoelastic dampers for structural applications. *Journal of Structural Engineering* 118: 1375–1392.